Available online at www.sciencedirect.com
SCIENCE DIRECT®
Physics Letters A 349 (2006) 306–313
PHYSICS LETTERS A
www.elsevier.com/locate/pla

Self-organized synchronization phenomena in a spatiotemporal coupled Lorenz model and its emergent abilities

Tetsuji Emura

College of Human Sciences, Kinjo Gakuin University, Omori 2-1723, Nagoya 463-8521, Japan

Received 31 March 2004; received in revised form 1 September 2005; accepted 15 September 2005

Available online 28 September 2005

Communicated by A.R. Bishop

Abstract

We propose a new spatiotemporal coupled Lorenz model that consists of three temporal coupling coefficients and three spatial coupling coefficients. And we find that self-organized phase transition phenomena appear in this model and manifestations of emergent abilities of this model through the implementation to the mutually connected neural networks.

PACS: 05.45.Xt; 05.45.Pq

Keywords: Coupled oscillator; On-off intermittency; Synchronization; Coincidence detector; Chaotic itinerancy; Neuron; Brain

1. Introduction

Recently, the phenomena of synchronization in coupled oscillator models have generated much interest in many area of mathematical physics [1,2], secure communications [3,4] and chemical biology [5]. Especially, a matter of great interest is the discovery of an evidence of synchronization phenomena of neurons in perceptive processes in the mammal's brain [6,7]. In addition, Inoue et al. [8] proposed a model of the processes in cognitive interpretation of the perception of necker's cube using the on-off intermittency [9,10] as appears in a coupled chaos oscillator. Further development of study for the coupled nonlinear oscillator models is expected from not only mathematical physics but also brain sciences [11], neural physiology [12] and neural computations [13].

On the other hand, the mutually connected neural networks are often used as a method of artificially making the associative memory that is one of the higher-order functions of human brain's behaviors. A system known well is the Hopfield network model proposed by J.J. Hopfield in 1982 [14]. If the Hopfield model is handled, original contents can be retrieved from imperfect information on memorized contents. This is a function that looks like the behavior of recollection of our memory: content-addressable memory [15], which is quite different from the computer of a so-called von Neumann type. However, the stage where contents are made to be memorized in the network and the stage where they are made to be retrieved are completely separated, it is difficult to say to simulate a higher-order function of our human brain.

Considering these situations, recently, the researches of the programmable neural networks [16] are advanced. In this study, we devise a new spatiotemporal coupled Lorenz model that consists of three temporal coupling coefficients $c_{1,2,3}$ and three spatial coupling coefficients $d_{1,2,3}$ and find that self-organized phase transition phenomena appear through the controlling of the values of $c_{1,2,3}$ and $d_{1,2,3}$, and that proposed model possesses the emergent abilities by the model is mounted in the mutually connected neural network systems. Then, we report because it was able to be confirmed that the systems can achieve the same kind of these function and it is an autonomous systems.

E-mail addresses: info@tetsujiemura.com, emura@kinjo-u.ac.jp (T. Emura).
URL: http://www.tetsujiemura.com.

0375-9601/$ – see front matter
doi:10.1016/j.physleta.2005.09.041

2. Coupled Lorenz model

Two continuous-time autonomous dynamical systems $\boldsymbol{X}_a$ and $\boldsymbol{X}_b$ are considered in n-dimensional Euclidean space $\boldsymbol{R}^n$, $\dot{\boldsymbol{X}}_a = \boldsymbol{F}(\boldsymbol{X}_a)$, $\dot{\boldsymbol{X}}_b = \boldsymbol{F}(\boldsymbol{X}_b)$. Here, $\boldsymbol{F}$ is considered to be the Lorenz system [17] for both with $n = 3$, $\boldsymbol{F} \stackrel{\text{def}}{=} (f_1\ f_2\ f_3)^T$, where individual vector components are $\boldsymbol{X}_a = (x_1\ x_2\ x_3)^T$, $\boldsymbol{X}_b = (x_4\ x_5\ x_6)^T$. These are bi-directionally coupled and indicated as below. Here, $0 < c < 1$ is a coupling coefficient.

$$\begin{pmatrix} \dot{x}_1 \\ \dot{x}_2 \\ \dot{x}_3 \end{pmatrix} = \begin{pmatrix} \sigma(x_2 - x_1) \\ x_1(r - x_3) - x_2 \\ x_1 x_2 - b x_3 \end{pmatrix} + c \begin{pmatrix} x_4 - x_1 \\ x_5 - x_2 \\ x_6 - x_3 \end{pmatrix}, \tag{1}$$

$$\begin{pmatrix} \dot{x}_4 \\ \dot{x}_5 \\ \dot{x}_6 \end{pmatrix} = \begin{pmatrix} \sigma(x_5 - x_4) \\ x_4(r - x_6) - x_5 \\ x_4 x_5 - b x_6 \end{pmatrix} - c \begin{pmatrix} x_4 - x_1 \\ x_5 - x_2 \\ x_6 - x_3 \end{pmatrix}. \tag{2}$$

In a mutually coupled oscillator system for Eqs. (1), (2), at least one of the maximum Lyapunov exponent for $\boldsymbol{F}$ is positive and the temporal coupling coefficient c is sufficiently small for $\boldsymbol{X}_a$ and $\boldsymbol{X}_b$, $\boldsymbol{X}_a$ and $\boldsymbol{X}_b$ depict independent trajectories, although when c is greater than certain value even if $|\boldsymbol{X}_a(0) - \boldsymbol{X}_b(0)| > 0$, the two trajectories are entrained bi-directionally and synchronized after a moment, the two then depict exactly the same trajectory. This means that the coupled oscillator system for Eqs. (1), (2) is in 6-dimensional space, although the two trajectories are constrained to 3-dimensional invariant manifold [2], and near this synchronous/desynchronous boundary, on-off intermittent chaos where the laminar phase and burst phase appear intermittently is observed at $\boldsymbol{X}_a(t) - \boldsymbol{X}_b(t)$. With in the laminar phase where the two trajectories are completely synchronized, an attractor is constrained to one plane of (x_1, x_3), identically, $x_1 - x_4$ becomes zero, which like the top figure of Fig. 1. These hyperplanes where attractor is constrained at the laminar phase are the (x_1, x_2) plane and (x_2, x_3) plane in addition to the (x_1, x_3) plane. In the $c = 0.4$, an attractor in the $(x_1 - x_4, x_2 - x_5, x_3 - x_6)$ space is indicated graphically in the bottom figure of Fig. 1. The trajectories the two are completely synchronized converge to one point of $(x_1 - x_4, x_2 - x_5, x_3 - x_6) = (0, 0, 0)$, although when on-off intermittent chaos occurs, they repeatedly have irregular and unpredictable intermittency with wandering into 3-dimensional space $(x_1 - x_4, x_2 - x_5, x_3 - x_6)$ from one point of $(0, 0, 0)$ like the bottom figure of Fig. 1.

3. A spatiotemporal coupled Lorenz model (STCL model)

The Lorenz model itself is a model of the smooth manifold in 3-dimensional space. When the coupled Lorenz attractor leaves invariant manifold, it simultaneously leaves the three hyperplanes. Thus, the author has considered this to be a model with three nonlinear oscillators: $\{\boldsymbol{X}, \boldsymbol{Y}, \boldsymbol{Z}\} = \{x_1 - x_4, x_2 - x_5, x_3 - x_6\}$ is coupled to each of the three by coupling of the coupled Lorenz model spatially as well and a new device was considered. This is indicated to the schematically in Fig. 2 and Eqs. (3) to (6), where $0 < c_{1,2,3} < 1$ are temporal coupling coefficients, $0 < d_{1,2,3} < 1$ are spatial coupling coefficients

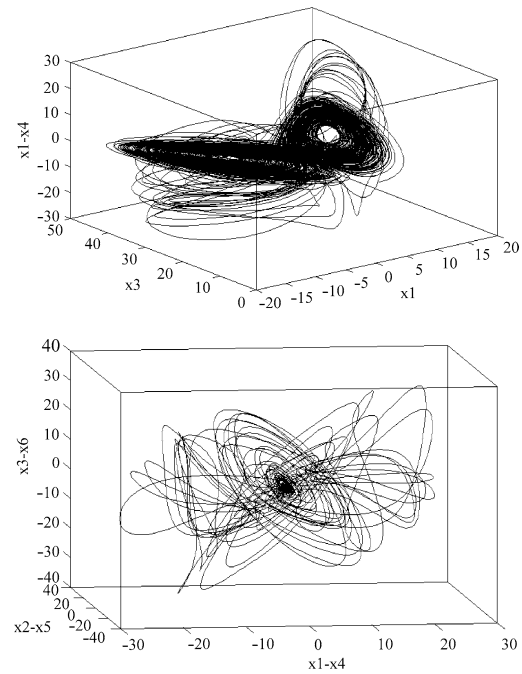

Fig. 1. An attractor of the coupled Lorenz model at $c = 0.4$, $t = 0$–250 [s], $\Delta t = 0.01$ [s]. Top: $x_1 - x_4$ versus (x_1, x_3) plane, bottom: $x_1 - x_4$ versus $x_2 - x_5$ versus $x_3 - x_6$, where $\sigma = 10$, $b = 8/3$, $r = 28$, $x_1(0) = x_2(0) = x_3(0) = 1.00$, $x_4(0) = x_5(0) = x_6(0) = 1.01$. (These are common specifications in this study.)

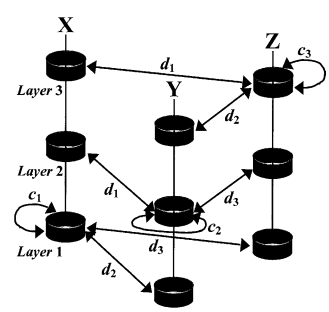

Fig. 2. Spatiotemporal coupled Lorenz model: a network model-based device, $\{\boldsymbol{X}, \boldsymbol{Y}, \boldsymbol{Z}\} = \{x_1 - x_4, x_2 - x_5, x_3 - x_6\}$.

$$\begin{pmatrix} \dot{x}_1 \\ \dot{x}_2 \\ \dot{x}_3 \end{pmatrix} = \begin{pmatrix} \sigma(x_2 - x_1) \\ x_1(r - x_3) - x_2 \\ x_1 x_2 - b x_3 \end{pmatrix} + \boldsymbol{D}^* \begin{pmatrix} x_4 - x_1 \\ x_5 - x_2 \\ x_6 - x_3 \end{pmatrix}, \tag{3}$$

$$\begin{pmatrix} \dot{x}_4 \\ \dot{x}_5 \\ \dot{x}_6 \end{pmatrix} = \begin{pmatrix} \sigma(x_5 - x_4) \\ x_4(r - x_6) - x_5 \\ x_4 x_5 - b x_6 \end{pmatrix} - \boldsymbol{D}^* \begin{pmatrix} x_4 - x_1 \\ x_5 - x_2 \\ x_6 - x_3 \end{pmatrix}, \tag{4}$$

$$\boldsymbol{D}^* = \boldsymbol{D} = \begin{pmatrix} c_1 & d_2 & d_3 \\ d_1 & c_2 & d_3 \\ d_1 & d_2 & c_3 \end{pmatrix}:$$

excitatory–excitatory connection, (5)

$$\boldsymbol{D}^* = \tilde{\boldsymbol{D}} = \begin{pmatrix} c_1 & d_2 & 1 - d_3 \\ 1 - d_1 & c_2 & d_3 \\ d_1 & 1 - d_2 & c_3 \end{pmatrix}:$$

excitatory–inhibitory connection. (6)

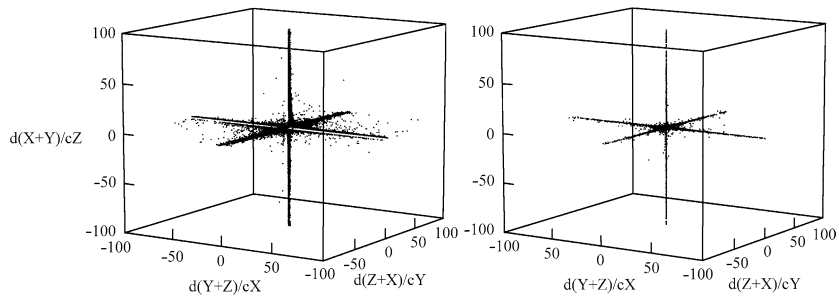

Fig. 3. Information distribution are plotted in horizontal $d(Z+X)/cY$ versus $d(Y+Z)/cX$ versus vertical $d(X+Y)/cZ$, left: $d/c = 0.3/0.23$, right: $d/c = 0.1/0.38$, where $t = 0$–1000 [s], $\Delta t = 0.01$ [s].

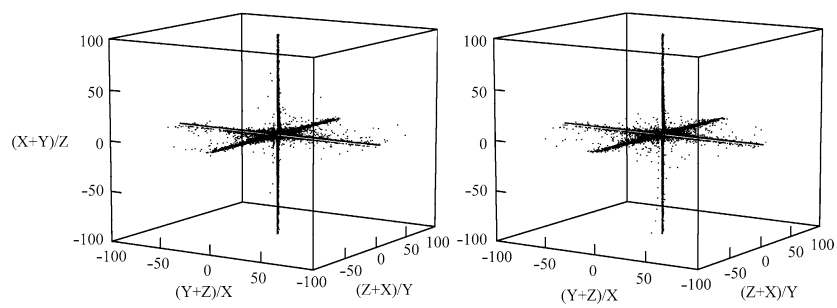

Fig. 4. Information distribution are plotted in horizontal $(Z+X)/Y$ versus $(Y+Z)/X$ versus vertical $(X+Y)/Z$, left: $d/c = 0.3/0.23$, right: $d/c = 0.1/0.38$, where $t = 0$–1000 [s], $\Delta t = 0.01$ [s].

First, the uniform spatial coupling coefficient $d_1 = d_2 = d_3 = d$ and the uniform temporal coupling coefficient $c_1 = c_2 = c_3 = c$ is considered. And c and d differ in order to examine the influence of c and d that affect the flow of information between the three nonlinear oscillators: $\{X, Y, Z\} = \{x_1 - x_4, x_2 - x_5, x_3 - x_6\}$ and the intermittency observed is almost the same, the ratio of c terms and d terms is plotted in Figs. 3 and 4. With regard to terms including the value of c and d like Fig. 3, the information flow between channels is greater with a larger d/c, although when plotting the same data without the value of c and d like Fig. 4, this difference is not noted for the most part. That is, the c and d control on-off intermittent chaos, although they have no direct effect on individual vectors. The c and d work as independent parameters without providing internal disturbance. Thus, the c and d are not constants and can be incorporated as coefficients that change with time and as functions of $\{X, Y, Z\}$. This indicates that they can be used as appropriate emergent parameters from the inside.

Next, the difference in behavior of the model with the case where the excitatory–excitatory connection matrix and the excitatory–inhibitory connection matrix is used are shown in Figs. 5 and 6. These figures show the behaviors of $\{x_1 - x_4, x_2 - x_5, x_3 - x_6\}$ to change of the values of d at the value of certain c. (Only $x_1 - x_4$ is illustrated in the figures. Each figure is plotted in $t = 0 \sim 10^5$ [s], $\Delta t = 0.01$ [s], $d = 0 \sim 1$. d is changing linearly with t where $d = 0.00001t$.)

When the excitatory–excitatory connection matrix is used (EEC model), as shown in Fig. 5, if the value of c becomes large, the value of d becomes small with which the $\{x_1 - x_4, x_2 - x_5, x_3 - x_6\}$ synchronizes, and an on-off intermittent domain also becomes narrow, then, d works as an effect like a switch. As shown in Fig. 6, when the excitatory–inhibitory connection matrix is used (EIC model), the domain of d separates to two places where the $\{x_1 - x_4, x_2 - x_5, x_3 - x_6\}$ does not synchronize. Furthermore, it should mention specially as shown in Fig. 6, in the domain of certain c, when only the value of d is changed, self-organized phase transition phenomena appear like: chaos phase → limit cycle phase → intermittent chaos phase → laminar phase.

4. Construction of emergent subsystems

4.1. Neural spike trains generator

In the proposed model, we regard the three nonlinear oscillators: $\{X, Y, Z\} = \{x_1 - x_4, x_2 - x_5, x_3 - x_6\}$ as three neurons. First, the synchronization phenomena are measured by the difference $\Delta_i(t) = |x_{i+3}(t) - x_i(t)|$, where $i = 1, 2, 3$. Next, the neurons are introduced using $\Delta_i(t)$ as

$$u_i(t) = \frac{1}{1 + \exp[-z_i(t)/z_0]}, \quad z_i(t) = \left(\frac{\varepsilon}{\Delta_i(t)}\right) - 1: \quad \text{analog model}, \tag{7}$$

where the state of $u_i(t)$ have the continuous value [0, 1] of the ith neuron at time t, z_0 is the analog parameter, and ε is the criterion parameter of the synchronization [18,19]. This analog neuron becomes the binary neuron $u_i(t)$ which have two states of $\{0, 1\}$ if $z_0 \to 0$ then

$$u_i(t) = \begin{cases} 1 & \text{if } \Delta_i(t) < \varepsilon, \\ 0 & \text{if } \Delta_i(t) \geqslant \varepsilon, \end{cases} \quad \text{digital model}. \tag{8}$$

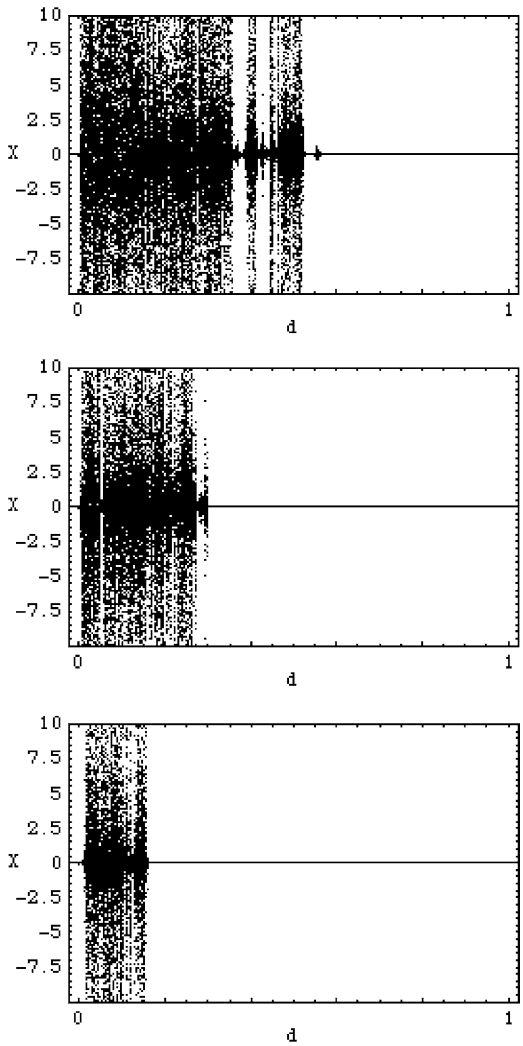

Fig. 5. $x_1 - x_4$ versus d, excitatory–excitatory connection, top to bottom, $c = 0.2$, $c = 0.3$, $c = 0.4$.

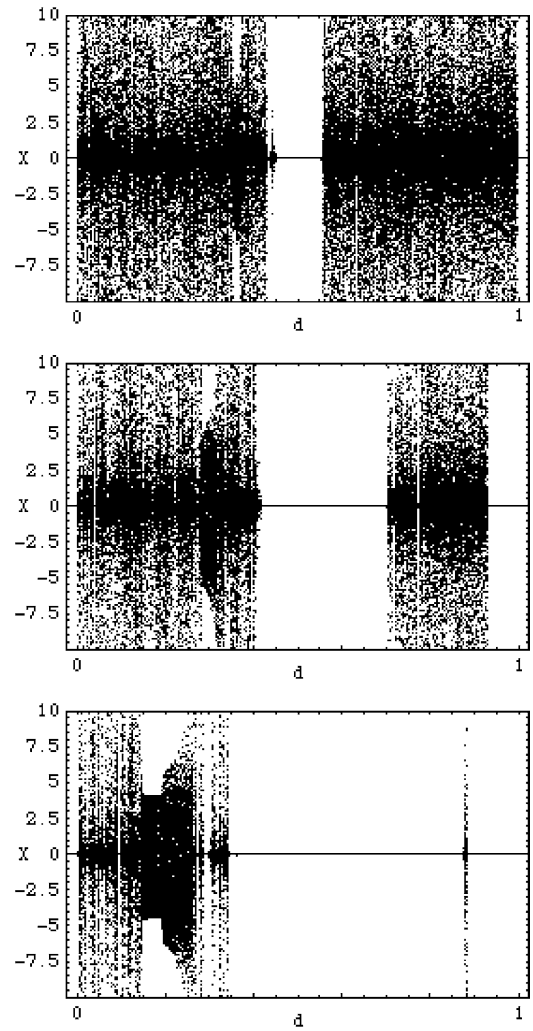

Fig. 6. $x_1 - x_4$ versus d, excitatory–inhibitory connection, top to bottom, $c = 0.2$, $c = 0.3$, $c = 0.4$.

4.2. Abstract coincidence detector model (ACD model)

Fujii et al. [20] have proposed an abstract coincidence detector model (ACD model). The essences of this model: (1) Each neuron is an excitatory neuron which does not have memory but fires by the simultaneity of a momentary incidence spike. (2) It does not have any inhibitory neuron. (3) Network structure does not assume any specific structure. (4) All synaptic weight is set to one. (5) A certain transfer delay time which exists beforehand is between neurons.

A schematic illustration of ACD model shows in Fig. 7, and we interpret this model to Eq. (9) when the above (5). is neglected, where $w_{i0} = 1$ and our model's $k = 3$.

$$D_i(t) = \begin{cases} 1 & \text{if } N = \sum_{i=1}^{k} w_{i0} u_i(t) = k \quad \text{or} \\ & \quad D = \prod_i w_{i0} u_i(t) = 1, \\ 0 & \text{if } N = \sum_{i=1}^{k} w_{i0} u_i(t) < k \quad \text{or} \\ & \quad D = \prod_i w_{i0}\, u_i(t) \neq 1. \end{cases} \tag{9}$$

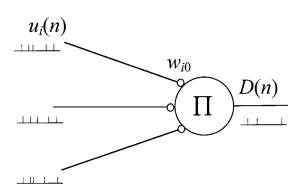

Fig. 7. Schematic illustration of ACD model.

4.3. Self-organized synchronization phenomena of EIC model

The spike trains are generated by using Eq. (8) from three neurons $\{X, Y, Z\}$, and the ACD output that is the output for them to have passed Eq. (9) is shown in Fig. 8 as the ratio of the number of all generated spikes to all calculated steps, and as the ratio of the number of synchronized spikes of three neurons to all generated spikes.

When Fig. 8 is compared with bottom figure of Fig. 6, three neurons $\{X, Y, Z\}$ have synchronized remarkably in the boundary regions of the limit cycle phase (which is a blank area in Fig. 8) and each chaos phases. In other words, a high information processing ability is potential in these regions. Therefore,

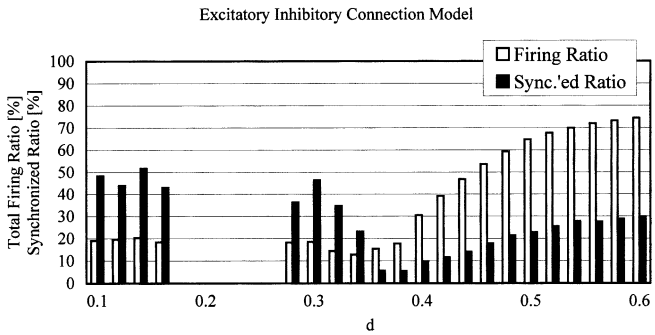

Fig. 8. Histogram of the ratio of the number of all generated spikes to all calculated steps (white-bar) and the ratio of the number of synchronized spikes of three neurons to all generated spikes (black-bar) versus d of the EIC model, $c = 0.4$, $t = 0$–1000 [s], $\Delta t = 0.01$ [s].

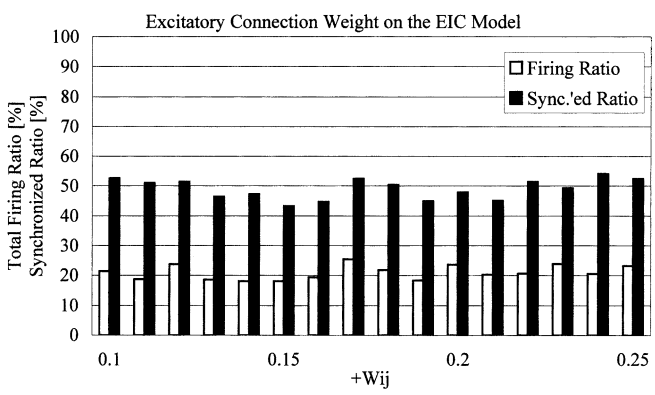

Fig. 9. Histogram of the ratio of the number of all generated spikes to all calculated steps (white-bar) and the ratio of the number of synchronized spikes of three neurons to all generated spikes (black-bar) versus w_{ij} of the EIC model, $c = 0.4$, $\theta_i = 0$, $t = 0$–1000 [s], $\Delta t = 0.01$ [s].

in our system, the spatial coupling coefficients d_i of the STCL model is regulated dynamically by the following way like the Hopfield model, when $c_i(t) = \text{const}$,

$$d_i(t) = \sum_{j=1}^{n} w_{ij}\, u_j(t) - \theta_i(t), \tag{10}$$

where $\theta_i(t)$ is the threshold value, w_{ij} $(= w_{ji})$ is the synaptic weight between ith and jth neurons and $w_{ii} = 0$.

Then, the difference of synchronization behavior by difference of the synaptic weight w_{ij} disappears almost according to this method as Fig. 9 shows. It is because the feedback of the spatial coupling coefficients $d_i(t)$ hang dynamically in chaotic attractor's behavior this is because the coefficients are controlled by using the ignitions of the neurons $\{X, Y, Z\}$.

5. Construction of emergent systems

5.1. DDN system and ADN system

Our emergent system is presented schematically in Fig. 10. The n subsystems (STCL models + ACD models) are connected to the external input of the mutually connected neural network through the connecting weight K_i with an external pattern. The state at the discrete time t of the ith neuron $v_i(t)$ is

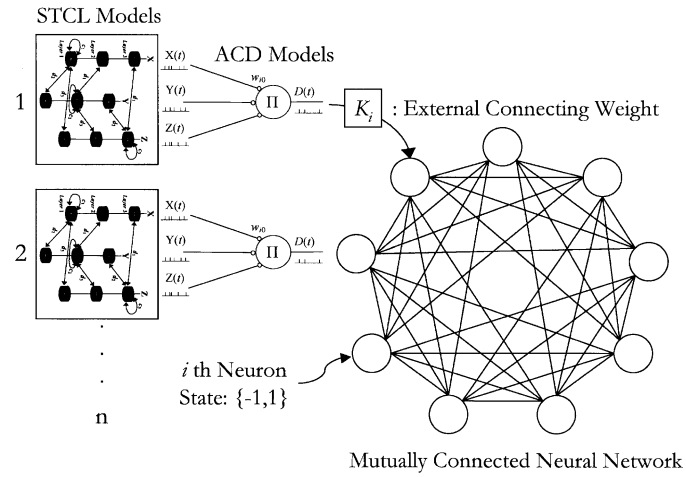

Fig. 10. Schematic illustration of the proposed emergent systems.

defined by

$$v_i(t+1) = \text{sign}\left[\sum_{j=1}^{n} J_{ij} v_j(t) + K_i k_i^{\text{ext}} S_i(t)\right], \tag{11}$$

$$S_i(t) = 2D_i(t) - 1. \tag{12}$$

The synaptic weight J_{ij} is given as the conventional autocorrelation associative memory,

$$J_{ij} = \begin{cases} \frac{1}{n}\sum_{\mu=1}^{p} \xi_i^{\mu}\xi_j^{\mu}\big(1 - \delta[i,j]\big), \\ J_{ji}, \end{cases} \tag{13}$$

to embed p patterns ξ^{μ}, where ξ_i^{μ} is the ith component of ξ^{μ} which takes binary value $\{-1, 1\}$, and this decision of J_{ij} is final. The k_i^{ext} is an external input pattern which takes binary value $\{-1, 1\}$ and $0 < K_i < 1$ is external connecting weight. The ξ_i^{μ} are vectors memorized in this network beforehand, however, k_i^{ext} is an unknown vector for the network. Here, $\text{sign}[x] = 1$ $(x \geqslant 0)$ or -1 $(x < 0)$, $\delta[i,j] = 1$ $(i = j)$ or 0 $(i \neq j)$.

There are two types in this system. One of these is a digital–digital network system (a DDN system) that is mounted to the digital subsystems which consist of digital neuron model of Eq. (8), another system is an analog–digital network system (an ADN system) that is mounted to the analog subsystems which consist of analog neuron model of Eq. (7). Both these types are auto-correlation type associative memory models. Even though having no learning synapse weight systems in these models, the models show several autonomous dynamics of retrieving embedded patterns by exciting an external input pattern from the subsystems. Next section shows these results.

5.2. Dynamics of the proposed systems

It shows the specifications for the numerical simulations. Concerning about n subsystems which take the EIC models; $\sigma = 10$, $b = 8/3$, $r = 28$, $c_1 = c_2 = c_3 = 0.4$, $d_{1,2,3} =$ variables, $w_{ij} = -1/3$, $\theta_i = -2/3$ and discrete time Δt for numerical simulations by Runge–Kutta method: $\Delta t = 0.01$ [s]. The criterion parameter takes $\varepsilon = 0.005$ at DDN system and

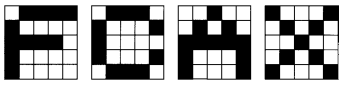

Fig. 11. Embedded patterns: ξ_i^μ, left to right, $\mu = 1, 2, 3$ and an external input pattern: k_i^{ext}.

$\varepsilon = 0.02$ at ADN system so that frequency of output spikes from subsystem might almost become equal to DDN system, and the analog parameter takes $z_0 = 0.01$. Concerning about a main system; number of neurons $n = 25$, number of embedded patters $p = 3$. These embedded patterns ξ_i^μ and an external input pattern k_i^{ext} show in Fig. 11. These vector are not orthogonal each other. And, this neural network system's feature is in the desynchronized neuron models. Therefore, we introduced a time delay $\tau_i = m \cdot i \cdot \Delta t$ in the each ith neuron. Now, in this report, it takes $m = 1$ and external connecting weight K_i takes constant value which is not depended by neuron index i.

The results are indicated in Figs. 12 and 13. First, concerning about Fig. 12 of DDN system, top figure which takes $K_i = 0.2$, the system behaves like an ordinary associative memory model. One of the embedded memory patterns is retrieved by initial conditions, and it is stabilized according to them. In this figure, this is a case of the system retrieved the pattern of $\mu = 1$. Next, bottom figure which takes $K_i = 0.9$, an external input pattern k_i^{ext} and this reversed pattern are repeated irregularly. Any embedded memory patterns are not retrieved. Of course, it finds also these same behaviors at ADN system. Concerning about Fig. 13, both of DDN system and ADN system which takes $K_i = 0.7$, all embedded memory patterns are irregularly retrieved by the external stimulation. Specifically, the embedded memory patterns $\mu = 1, 2, 3$ are retrieved at $t = 2, 10, 32$ [s], respectively in the DDN system, and $t = 5, 12, 96$ [s], respectively in the ADN system. Moreover, the several new patterns which the embedded memory patterns and the external input patterns compounded are also generated.

What should make a special mention here, the synaptic connection weight J_{ij} on the network has not been renewed in this model at all. Generally, in the associative memory systems, if some learning algorithms are not added to Eq. (13) by using the plasticity of the synapse to retrieving two or more embedded vectors in the time series, such as autonomous dynamics of retrieving are not caused. This proposed system is a model of the autocorrelation associative memory. However, these embedded patterns can be made unstable by external stimulation. In other words, the trajectories cannot stay for a long time by one attractor and wander between these embedded attractors by external stimulation which is generated by subsystems that consist of STCL models plus ACD models. This is a phenomenon that looks like "chaotic itinerancy" that Tsuda [21] discovered. Moreover, it was a system in the research of Aihara et al. [22] based on the nerve model though a similar phenomenon was cited. However, the Lorenz chaos of this model is quite unrelated to neurophysiology. It is suggested that these phenomena are not only the chaos of the nervous systems but also universal characteristics of the chaos that is generated by coupled nonlinear oscillator systems.

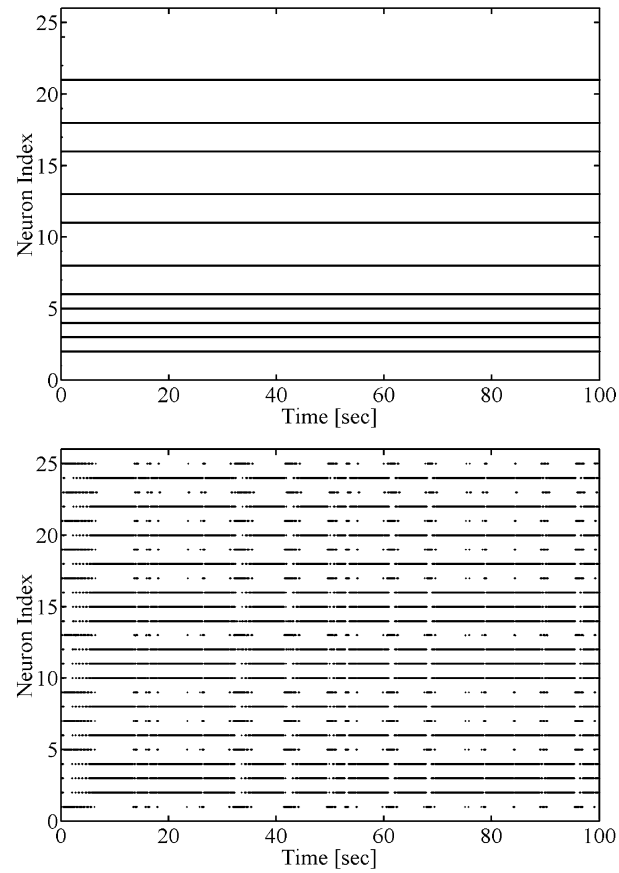

Fig. 12. Retrieving pattern dynamics of DDN system ($\varepsilon = 0.005$), $t = 0$–100 [s]. Top: $K_i = 0.2$, bottom: $K_i = 0.9$.

Next, we investigated the influence that the difference of the criterion parameter ε gave to this network. The output of the subsystem as the external stimulation give an unknown vector is one spike train to which the spike that synchronizes spatially is taken out by using the ACD model from the three trains fired from the STCL model. The parameter that decides the threshold that generates these spike trains is ε in the STCL model. What influence does the value of ε give to this network? Fig. 14 is the same condition as Fig. 13 excluding ε. And, the value of ε was widened from 0.005 to 0.02 for the DDN system, and the value of ε was widened from 0.02 to 0.04 for the ADN system.

It is understood that the network does not react to it though external stimulation is input when ε is widened as this Fig. 14 shows. In other word, this network model's recollection does not depend on an arbitrary external input spike train but it is certainly driven by synchronous phenomenon of the three neurons $\{X, Y, Z\}$ in subsystems.

6. Summary

We proposed a new Lorenz model with an excitatory–excitatory connection matrix (EEC model) or an excitatory–inhibitory connection matrix (EIC model) which consists of the three temporal coupling coefficients $c_{1,2,3}$ and three spatial coupling coefficients $d_{1,2,3}$. This spatiotemporal coupled Lorenz model is a model that synchronizes three nonlinear oscillators.

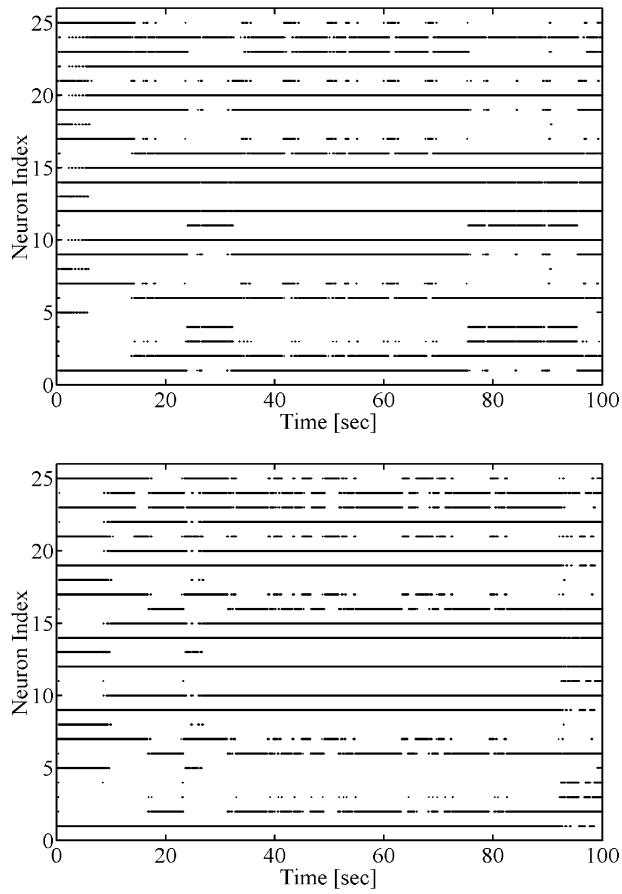

Fig. 13. Retrieving pattern dynamics at $K_i = 0.7$, $t = 0$–100 [s]. Top: DDN system ($\varepsilon = 0.005$), bottom: ADN system ($\varepsilon = 0.02$).

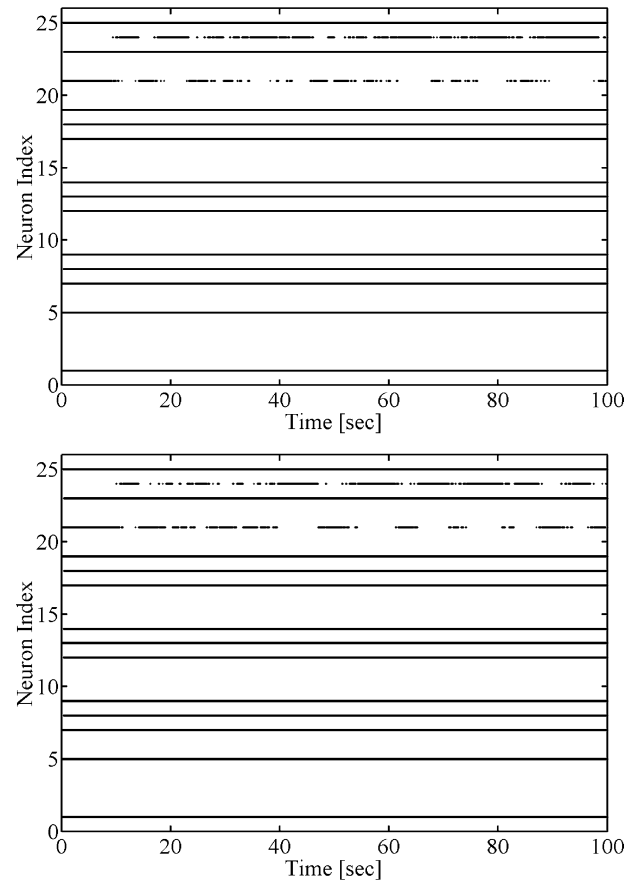

Fig. 14. Retrieving pattern dynamics at $K_i = 0.7$, $t = 0$–100 [s]. Top: DDN system ($\varepsilon = 0.02$), bottom: ADN system ($\varepsilon = 0.04$).

The $c_{1,2,3}$ and $d_{1,2,3}$ are parameters independent of each term's vector, and on-off intermittency observed in this model is controlled by $c_{1,2,3}$ and $d_{1,2,3}$. In this study, we discover that self-organized phase transition phenomena appear in this model in changing the values of $c_{1,2,3}$ and $d_{1,2,3}$.

We introduced an abstract coincidence detector model (ACD model) to evaluate the spatial synchronization of neurons, and introduced the Hopfield model to decide the three spatial coupling coefficients $d_{1,2,3}$ which govern emergent abilities. It showed that boundary regions of each phase of the self-organized phase transition phenomena which appear in the proposed model have information processing ability, and claimed that a proposed model is useful to an architecture for emergent subsystems for implementation of an emergent system.

We proposed an emergent system that is a mutually connected neural network model which is mounted to the spatiotemporal coupled Lorenz model-based subsystems. There are two types in this system. One of these is a digital–digital network system (a DDN system), another model is an analog–digital network system (an ADN system). Both these types are auto-correlation type associative memory model. Even though having no learning synapse weight systems in these systems, the models show several autonomous dynamics of retrieving embedded patterns by stimulating an external input pattern from the subsystems.

7. Outlook

In next paper, we will propose a model of controlling of the proposed system that is called "self-reference model". It is indicated to Eq. (14) which is modified based on Eq. (12). Here, st_1 and st_2 are specifications of the model.

$$S_i(t) = \begin{cases} 2D_i(t) - 1 & \text{if } t \leqslant st_1, \\ v_i(t) & \text{if } st_1 < t \leqslant st_2, \\ 2D_i(t) - 1 & \text{if } st_2 < t. \end{cases} \tag{14}$$

By using this model, we have found a dynamics of the proposed system quite changing after the self-reference. We will report the detail in next paper.

Acknowledgements

This work was supported by special research grant from the Kinjo Gakuin University.

References

[1] H. Fujisaka, T. Yamada, Prog. Theor. Phys. 69 (1983) 32.
[2] E. Ott, J.C. Sommerer, Phys. Lett. A 188 (1994) 39.
[3] L.M. Pecora, T.L. Carroll, Phys. Rev. Lett. 64 (1990) 821.
[4] L. Kocarev, U. Parlitz, Phys. Rev. Lett. 77 (1996) 2206.
[5] S.K. Han, C. Kurrer, K. Kuramoto, Phys. Rev. Lett. 75 (1995) 3190.
[6] C.M. Gray, P. König, A.K. Engel, W. Singer, Nature 338 (1989) 334.

[7] C.M. Gray, W. Singer, Proc. Natl. Acad. Sci. USA 86 (1989) 1698.
[8] M. Inoue, K. Nakamoto, Prog. Theor. Phys. 92 (1994) 501.
[9] H. Fujisaka, T. Yamada, Prog. Theor. Phys. 74 (1985) 918.
[10] N. Platt, E.A. Spiegel, C. Tresser, Phys. Rev. Lett. 70 (1993) 279.
[11] C.A. Skarda, W.J. Freeman, Behavioral Brain Sci. 10 (1987) 161.
[12] Y. Asai, et al., Biol. Cybern. 88 (2003) 152.
[13] P. König, T.B. Schilen, Neural Computation 3 (1991) 155.
[14] J.J. Hopfield, Proc. Natl. Acad. Sci. USA 79 (1982) 2554.
[15] J.J. Hopfield, Proc. Natl. Acad. Sci. USA 81 (1984) 3088.
[16] M. Watanabe, K. Aihara, S. Kondo, Biol. Cybern. 78 (1998) 87.
[17] E.N. Lorenz, J. Atmos. Sci. 20 (1963) 130.
[18] M. Inoue, A. Nagayoshi, Phys. Lett. A 158 (1991) 373.
[19] M. Inoue, K. Nagayoshi, Prog. Theor. Phys. 88 (1992) 769.
[20] H. Fujii, et al., Neural Networks 9 (1996) 1303.
[21] I. Tsuda, Neural Networks 5 (1992) 313.
[22] M. Adachi, K. Aihara, Neural Networks 10 (1997) 83.